Food & Function

ROYAL SOCIETY OF CHEMISTRY

PAPER

View Article Online
View Journal | View Issue

Cite this: *Food Funct.*, 2024, **15**, 2655

Screening and molecular dynamics simulation of ACE inhibitory tripeptides derived from milk fermented with *Lactobacillus delbrueckii* QS306

Nan Wu, [a] Puyu Li,[a] Quan Shuang*[a] and Wuhanqimuge *[b]

Peptides in milk fermented with *Lactobacillus delbrueckii* QS306 before and after ultrahigh pressure treatment were identified using proteomics. Subsequently, 16 stable tripeptides were screened out based on activity score prediction, PeptideCutter analysis, and hydrophobicity calculations. Among them, WRP, WSR, and YRP showed the best angiotensin-converting enzyme (ACE) inhibitory activity, and their semi-inhibitory concentrations were 46.707, 300.121, and 89.555 μM, respectively. WRP and WSR were competitive inhibitors, whereas YRP was non-competitive. Gastrointestinal simulation revealed that WRP and YRP had better gastrointestinal stability. The values of RMSD, ΔG_{bind}, ΔG_{pol}, and RSMF obtained from molecular dynamics simulation indicated that the interaction of WRP and ACE was stable. Thus, *Lactobacillus delbrueckii* QS306-fermented milk can serve as an important source of ACE inhibitory peptides both before and after ultrahigh pressure treatment. The strategy of *in silico* screening, activity evaluation, and molecular dynamics simulation adopted in this study can be applied to the large-scale screening of novel peptides with high ACE inhibitory activity.

Received 11th August 2023,
Accepted 19th January 2024

DOI: 10.1039/d3fo03320a

rsc.li/food-function

1. Introduction

Milk and dairy products have become increasingly popular as nutritious foods because of their rich nutritive value and easy digestion and absorption. For humans, milk and dairy products are important sources of calcium, phosphorus, proteins, vitamin A, vitamin B2, and vitamin D.[1] Studies have shown that dairy products can lower blood pressure;[2] produce DPP-IV inhibition;[3] and exert antioxidative,[4] anticancer,[5] and immunomodulatory effects.[6]

Hypertension is a serious disorder and increases the risk of cardiovascular, neurological, and renal diseases, among others. Hypertension is also the main cause of premature death worldwide.[7] Therefore, the effective control of hypertension is required to attenuate its effects on human health. Hence, in clinical settings, chemically synthesized drugs are used to control blood pressure. However, their long-term and combinatorial use can induce adverse reactions such as arrhythmia,[8] muscle spasm, dry cough,[9] blurred vision, and asthma. Given that dairy products are regularly consumed by humans, their value as a source of natural angiotensin-converting enzyme (ACE) inhibitory peptides that are non-toxic and have no adverse effects has attracted widespread attention.

ACE inhibitory peptides were first obtained from venomous snakes[10] and were then discovered in several types of food proteins. Fermented milk protein is an important source of such peptides. Two tripeptides VPP and IPP purified from milk fermented by *Lactobacillus helveticus* JCM 1004 previously showed strong antihypertensive effects.[11] One study aimed to enhance the ACE inhibitory activity of fermented milk by increasing its protein content and utilizing *Lactobacillus helveticus* LH-B02, achieving the release of bioactive peptides.[12] Another study showed that the peptides isolated from milk fermented by *Lactobacillus helveticus* NCDC 288 have ACE inhibitory activity *in vitro*.[13] A novel ACE inhibitory peptide released from camel milk by *Lactobacillus acidophilus* NCDC-15 was effectively hydrolyzed in an earlier study, and *Lactobacillus acidophilus* NCDC-15 showed good PepX activity and ACE inhibitory activity.[14] Peptides with strong antihypertensive properties were also identified in goat milk fermented by *Lactobacillus bulgaricus* LB6;[15] milk fermented by *Lactobacillus rhamnosus* GG and *Streptococcus thermophilus* SY-102;[16] and milk fermented by *Pediococcus pentosaceus*, goat milk, sheep milk, and camel milk.[17] During this search for ACE inhibitory peptides, research methods for their identification and development have been constantly changing and improving.

[a]*Department of College of Food Science and Engineering, Inner Mongolia Agricultural University, Hohhot, Inner Mongolia, 010018, People's Republic of China. E-mail: shuangquan@imau.edu.cn; Fax: +86-10-4305350; Tel: +15849166155, +86-10-4305350*

[b]*Experimental center, Inner Mongolia Traditional Chinese & Mongolian Medical Research Institute, Hohhot, Inner Mongolia, 010017, People's Republic of China. E-mail: 939839367@qq.com; Fax: +86-10-4961482; Tel: +18047119596, +86-10-4961482*

In early research, peptide separation and identification were mainly performed using ultrasonic treatment, ultrafiltration, concentration chromatography, electrophoresis, and high-performance liquid chromatography. With these methods, it was difficult to identify peptides with high time consumption, small molecular weight, and low concentrations. With the evolution of scientific methods, mass spectrometry is now applied to identify analyte sequences, and BIOPEP-UWM and PeptideRanker are used as bioinformatics databases, software, and tools to analyze the ACE inhibitory peptides in a protein, perform computerized protein hydrolysis, and predict peptide activity, structure–activity relationships, and physicochemical properties.[18] In addition, molecular docking has emerged as a valuable tool for screening and designing ACE inhibitory peptides and is widely used to elucidate interaction mechanisms.[19]

Previous studies have shown that the ACE inhibitory activity of milk fermented by *Lactobacillus delbrueckii* QS306 increases significantly after ultrahigh pressure treatment.[20] In this study, UPLC-Q-exactive-HF-X-MS/MS was used to identify the peptides in whey fermented by *Lactobacillus delbrueckii* QS306 before and after ultrahigh pressure treatment. Subsequently, potential ACE inhibitory tripeptides were screened out using bioinformatics methods, and the activity of predicted tripeptides showing good stability was verified. Further, their *in vitro* stability was also tested. The binding mode of tripeptides was explored using Lineweaver–Burk plots, and the binding mechanism between the tripeptides and ACE was explored using molecular docking and molecular dynamics simulation.

2. Materials and methods

2.1 Materials

L. delbrueckii QS306 was isolated from traditionally fermented milk (Xilin Gol League, China). Angiotensin-converting enzyme (ACE), hippuric acid (HA), and *N*-benzoyl-Gly-His-Leu (*N*-hippuryl-His-Leu hydrate; HHL, powder, H1635) were purchased from Sigma-Aldrich Chemical Co. (Saint Louis, MO, USA). Simulated gastric fluid and intestinal fluid were obtained from Yuanye Biotechnology Co., Ltd (Shanghai, China).

2.2 Preparation and ultrafiltration of fermented milk

L. delbrueckii QS306 was grown in MRS (Guangdong Huankai Microbial Sci. & Tech. Co, Guangzhou, China). The strain was activated (37 °C for 24 h) and centrifuged (3500*g* for 10 min). The cell pellet was resuspended in sterile saline. Cell suspension (3%, v/v) was added to sterile reconstituted skim milk (11%, w/v), followed by incubation at 37 °C for 48 h, to obtain FM.

FM was treated under ultra-high pressure (HPP 600 MPa per 30 L, Baotou Kefa High Pressure Tech. Co., Ltd, Baotou, China) at 400 MPa for 10 min to obtain UHP-FM. The pH of FM and UHP-FM was adjusted to 4.6, and the samples were centrifuged (3000*g*, 4 °C, 15 min). The supernatant was collected in a 3 kDa ultrafiltration centrifuge tube (Amicon Ultra-15 mL, Millipore, Billerica, USA) and centrifuged (3000*g*, 4 °C, 30 min), and fractions with a molecular weight (MW) < 3 kDa were obtained.

2.3 Identification of peptide sequences

The ultrafiltered samples were subjected to desalting. They were eluted using an UPLC-Q-exactive-HF-X-MS/MS mass spectrometer (Easy nLC 1200, Thermo Fisher Scientific Inc., Waltham, MA). Data were analyzed using MaxQuant 1.6.1.0 software[21] and the *Bos Taurus* (Bovine) UniProt protein database [9913]-46728-20201102.

2.4 Stability prediction and simulation of short peptide synthesis

PeptideCutter (**https://web.expasy.org/peptidecutter/**) was used to predict the results of simultaneous protein hydrolysis by a single protease and multiple proteases. PeptideCutter was used to simulate the digestion of newly identified peptides with activity scores >0.6 (**https://distilldeep.ucd.ie/PeptideRanker/**) and hydrophobicity >7.0.[22] Fmoc solid-phase synthesis was performed by Gil Biochemical (Shanghai, China) Co., Ltd.

2.5 ACE inhibition activity assay and peptide inhibition pattern

Each peptide (40 μL) was treated with HHL (80 μL, 0.5 mM) at 37 °C for 5 min and then treated with ACE (40 μL, 0.1 U mL^{-1}). The mixture was incubated at 37 °C for 60 min, followed by the addition of HCl (200 μL, 1.0 mol L^{-1}) to discontinue the reaction. The control included BBS (40 μL, pH 8.3) instead of peptides. The peak area of HA produced after the reaction was determined using a 10 μL reaction solution. The ACEI rate of the peptides was calculated using the following formula:

$$\text{ACE inhibition } (\%) = [(A_{\text{control}} - A_{\text{inhibitor}})/(A_{\text{control}}) \times 100]$$

The inhibition patterns of peptides were determined based on a previously described method.[23] The inhibition pattern of the peptides was determined using Lineweaver–Burk plots. The slope of the Lineweaver–Burk plot was taken as the *Y* axis, and the peptide concentration was taken as the *X* axis. The inhibition constant (K_i) was the intercept on the *X* axis.

2.6 Molecular docking

Molecular docking was used to analyze the low-energy binding mode of the ligands and receptor active sites. Thus, it could further explain the mechanism of binding between ACEI peptides and ACE. Using Discovery Studio 2019 software, the molecular structure of the short peptides was constructed. The crystal structure of ACE (PDB:1O8A) was downloaded from the PDB (**https://www.rcsb.org/**) database. The active coordinate sites were defined as *X*: 36.4297, *Y*: 37.2927, and *Z*: 42.4473, and the docking radius was 15 Å.

2.7 *In vitro* digestion simulation

A pepsin–trypsin *in vitro* system simulating gastrointestinal digestion was used as described previously,[24] with slight modi-

fications. Briefly, each peptide (1 mg mL^{-1}) was treated with simulated gastric fluid (4%, pH 2) in a water bath shaker (65 rpm) at 37 °C for 2 h. Further, the pH of the solution was adjusted to 7.5, and simulated intestinal fluid (4%, pH 7.5) was added. The solution was incubated on a water bath shaker (65 rpm) at 37 °C for 3 h, and samples were collected every 30 min. The peptides were inactivated by heating at 95 °C for 10 min. The solution pH was adjusted to 8.3 to determine ACEI activity. The peptide-digesting effect of the simulated gastric fluid and intestinal fluid was assessed.

2.8 Molecular dynamics

Molecular dynamics (MD) simulations were performed using the GROMACS (**https://www.gromacs.org**) program. The Ante Chamber Python parser interface (ACPYPE) in Amber Tools v18 was used to parameterize the topology, atomic type, and charge required for small molecules. The Amber99sb-ildn force field was applied to all simulations. SPC216 water molecules were added to the dodecahedron, Na^+, and Cl^- to balance the charge in the system to neutral, and energy minimization (EM) was also performed. Further, the system was heated to 310.15 K in 1 fs time steps during the 200 ps NVT simulation, and the pressure was balanced to 1 atmosphere in 2 fs time steps during the 100 ps NPT simulation. For the 80 ps MD simulation, a well-balanced system with constant pressure was released and constrained, and a jump algorithm was further used to achieve a simulation balance of 100 ns in steps of 2 fs. The particle grid Ewald summation method with 0.16 grid spacing was used to calculate long-distance electrostatic interactions, and the parallel LINCS method was used to constrain the hydrogen bonds during the equilibrium process. Finally, MD simulation was performed. During the simulation run, the entire trajectory was saved for analysis at a frequency of 100 ps. To evaluate the dynamic and static interactions of the complex, the MD trajectory was analyzed using the following parameters: root mean square deviation (RMSD), root mean square fluctuation (RMSF), β factor, hydrogen bond number (H bond), free energy landscapes (FEL), and binding pattern.

2.9 Calculation of free energy of binding

The free energy of molecular binding is a very important physical parameter indicating the affinity of a protein to a ligand. In this study, the Molecular Mechanics Poisson–Boltzmann surface area (MM-PBSA) method was used to estimate the free energy of binding. The free energy of binding (ΔG_{bind}) using the g_mmpbsa method. ΔG_{bind} was calculated as a combination of van der Waals (ΔG_{vdw}), electrostatic (ΔG_{ele}), polar (ΔG_{polar}), and nonpolar solvent (ΔG_{nonpol}) energies.

2.10 Data statistics and analysis

The data were expressed as mean ± standard deviation (SD). GraphPad Prism 9.0 (GraphPad Software Inc., La Jolla, CA, USA) and Microsoft Excel 2020 (Microsoft Co., USA) software were used to generate graphs. All the obtained data were subjected to analysis of variance (ANOVA) using SPSS software (version 19; IBM).

3 Results and discussion

3.1 Identification of the ACE inhibitory activity of peptides

After UHP treatment, the ACE inhibitory activity of the MW < 3 kDa fraction of whey in milk fermented with *Lactobacillus delbrueckii* QS306 (obtained *via* ultrafiltration separation) was significantly higher (98.95 ± 0.65%) than that of the fraction from untreated whey (89.46 ± 0.790%). The MW < 3 kDa fractions from UHP-FM and FM were analyzed and sequenced using peptidomics. The protein source, relative molecular mass, potential activity score, hydrophobicity, isoelectric point, and sample source of the 566 short peptides from UHP-FM and FM were analyzed. Of the 566 peptides, 170 were novel tripeptides (Fig. 1A). Among them, 75 tripeptides had activity scores >0.6 and hydrophobicity >7 kJ mol^{-1} (Table 1) and were derived from 11 kinds of proteins (Fig. 1B). Notably, 40 tripeptides were detected in FM and UHP-FM. Among them, the most common tripeptides were those belonging to Spectrin repeat containing nuclear envelope protein 2, Dynein axonemal heavy chain 9, Alpha-S1-casein, Beta-casein, Uncharacterized protein, and Midasin. Interestingly, the Midasin protein exists in many organisms and is involved in protein hydrolysis, protein folding, protein unfolding, membrane transport, and the assembly of macromolecular complexes in the nucleus.[25] Alpha-S1-casein and Beta-casein are the main proteins in milk.

Then, the stability of the 75 tripeptides was predicted using PeptideCutter, and it was found that only 16 tripeptides were not easily decomposed by pepsin and trypsin. Then, these 16 tripeptides (HGF, MMS, MMT, NPW, PMH, PPF, SWM, WMG, WPR, WRP, WSM, WSR, YGR, YPQ, YRP, and YPY) were synthesized in their solid state, and their ACE inhibitory activities were determined (Fig. 1C). The ACE inhibitory activities of MMS, MMT, WPR, WRP, WSM, WSR, and YPY were found to be 96.50 ± 0.94%, 94.55 ± 0.52%, 91.36 ± 0.53%, 98.50 ± 1.3%, 88.59 ± 0.59%, 95.56 ± 0.15%, and 98.18 ± 0.12%, respectively. Subsequently, the ACE semi-inhibitory concentrations (IC_{50}) of these tripeptides were determined (Fig. 1D). Among them, WRP, WSR, and YRP had the best ACE inhibitory activities, with IC_{50} values of 46.707 μM, 300.121 μM, and 89.555 μM, respectively. FM contained the ACE inhibitory peptides WSR, YRP, and WRP, whereas UHP-FM only contained YRP. Hydrophobic peptides can easily cross the cell membrane of target organs, and the presence of specific terminal amino acids (Tryptophan [W], Phenylalanine [F], Histidine [H], Proline [P], Methionine [M], and Tyrosine [Y]) enhances their electron-donating ability. The presence of positively charged amino acid P residues or F, W, and Y at the C terminal improves the hydrolysis of angiotensin-I and induces stronger ACE inhibition. The ACE inhibitory potential of a peptide is influenced by the charged amino acids at its N- or C-terminal.[26] In particular,

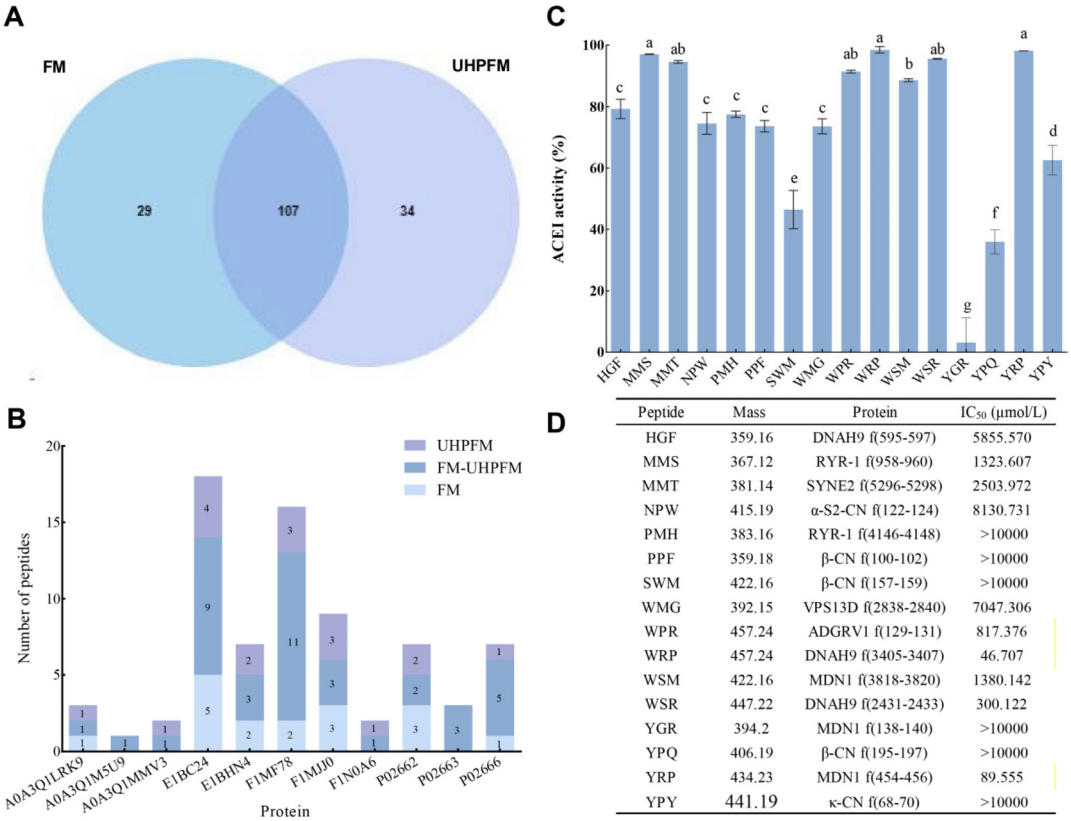

Peptide	Mass	Protein	IC_{50} (μmol/L)
HGF	359.16	DNAH9 f(595-597)	5855.570
MMS	367.12	RYR-1 f(958-960)	1323.607
MMT	381.14	SYNE2 f(5296-5298)	2503.972
NPW	415.19	α-S2-CN f(122-124)	8130.731
PMH	383.16	RYR-1 f(4146-4148)	>10000
PPF	359.18	β-CN f(100-102)	>10000
SWM	422.16	β-CN f(157-159)	>10000
WMG	392.15	VPS13D f(2838-2840)	7047.306
WPR	457.24	ADGRV1 f(129-131)	817.376
WRP	457.24	DNAH9 f(3405-3407)	46.707
WSM	422.16	MDN1 f(3818-3820)	1380.142
WSR	447.22	DNAH9 f(2431-2433)	300.122
YGR	394.2	MDN1 f(138-140)	>10000
YPQ	406.19	β-CN f(195-197)	>10000
YRP	434.23	MDN1 f(454-456)	89.555
YPY	441.19	κ-CN f(68-70)	>10000

Fig. 1 Source and ACE inhibitory activity of tripeptides present in FM and UHP-FM (A: VENN diagram of tripeptides present in FM and UHP-FM; B: VENN diagram of tripeptides with potential ACE inhibitory activity present in FM and UHP-FM; C: ACE inhibitory activity of stable tripeptides predicted by PeptideCutter; D: molecular weights, protein sources, and semi-inhibitory concentrations of the tripeptides).

N-terminal aliphatic amino acids and C-terminal aromatic amino acids with Proline at the third or fourth position from the C-terminal can actively chelate zinc atoms at the active site of ACE, making it inactive.[27]

3.2 Determining ACE inhibition patterns

In order to determine the mode of ACE inhibition, Lineweaver–Burk diagrams were generated. Kinetic studies were conducted in the presence and absence of 10 and 30 μM WRP peptides, 50 and 100 μM WSR peptides, and 20 and 40 μM YRP peptides. Although the V_{max} effect of WRP and WSR did not change, the K_m value changed. These findings were suggestive of a competitive inhibition mode (Fig. 2B and C). Most ACE inhibitory peptides show competitive inhibition. The K_m of the control (without peptide) was 3.228 mM. However, in the presence of 10 and 30 μM WRP, the K_m increased to 5.099 and 9.597 mM, respectively. Similarly, in the presence of 50 and 100 μM WSR, the K_m increased to 5.959 and 14.148 mM, respectively. Together, these results showed that WRP and WSR inhibit the enzyme by binding to the free enzyme instead of the ACE–substrate complex. Since the inhibitory pattern of ACE inhibitory peptides is related to their structures, we speculate that the peptides may have a similar structure to ACE substrates. Therefore, they may compete with the substrate and bind to the same interaction site within the enzyme. Notably, the K_m value did not change in the presence of YRP, although the V_{max} value was altered, indicating that non-competitive inhibition had occurred (Fig. 2A). The V_{max} value of the control (without peptide) was 13.323 g mL^{-1} min, but the V_{max} decreased to 8.375 and 1.581 μg mL^{-1} min in the presence of 20 and 40 μM of the YRP peptide. This shows that peptides can bind to enzymes to form dead-end complexes.[28] This also suggests that peptides can bind to substrates at different sites, reducing the efficiency of enzyme catalysis by forming enzyme–substrate–inhibitor and enzyme–inhibitor complexes. The K_i represents the binding affinity of a short peptide with ACE.[29] Higher K_i values are representative of lower affinities of the ACE inhibitory peptides to ACE. The inhibitory constants K_i of the WRP, WSR, and YRP peptides were 14.29, 20.71, and 0.091 μM, respectively. The ACE inhibitory activity of the tripeptides (YRP > WRP > WSP) was consistent with the inhibition curve.

3.3 *In vitro* simulated gastro-intestinal digestion

Bioactive peptides must survive after digestion in the gastrointestinal tract and maintain their structure and activity when they reach their targets. In order to evaluate the resistance of WRP, WSR, and YRP to digestive enzymes such as pepsin and trypsin, which are the main digestive proteases in the gastrointestinal tract, the peptides were hydrolyzed separately and

Table 1 Screening of tripeptides in fermented milk (FM) and ultra-high-pressure-treated FM (UHP-FM) based on hydrophobicity and activity

UniProt AC	Protein	Peptides	Mass	Activity	Hydrophobicity (Q)	PI	Toxicity	FM/ UHP-FM
A0A3Q1LRK9	Dynein axonemal heavy chain 11	PHF	438.21	0.94	8.56	7.17	NT	+*
		WFK	399.19	0.98	11.09	8.75	NT	**
		WVP	479.25	0.87	11.63	5.52	NT	*+
A0A3Q1M5U9	Kappa-casein	YPY	441.19	0.74	12.72	5.52	NT	**
A0A3Q1MMV3	Ryanodine receptor 1	FFR	422.23	0.99	8.96	9.75	NT	**
		RFP	410.22	0.98	8.67	9.75	NT	+*
E1BC24	Midasin	FAK	422.23	0.62	8.3	8.75	NT	+*
		MLH	431.23	0.67	6.17	6.49	NT	+*
		MLW	422.16	0.98	10.49	5.28	NT	+*
		PFK	364.21	0.86	10.28	9.18	NT	*+
		RFA	415.22	0.87	6.72	9.75	NT	*+
		RFT	484.23	0.76	6.12	9.75	NT	**
		RPF	418.23	0.98	8.67	9.75	NT	*+
		RPP	450.26	0.86	8.3	9.75	NT	**
		VLF	434.23	0.73	10.57	5.49	NT	**
		WAR	440.23	0.9	7.81	9.75	NT	*+
		WRQ	390.23	0.83	6.21	9.75	NT	**
		WSM	462.28	0.95	8.04	5.52	NT	+*
		YGR	448.21	0.68	6.87	8.75	NT	**
		YLR	377.23	0.56	8.96	8.75	NT	**
		YRG	553.33	0.67	6.87	8.75	NT	*+
		YRL	524.3	0.64	8.96	8.75	NT	**
		YRP	538.32	0.77	9.14	8.75	NT	**
		YWL	506.25	0.95	12.63	5.52	NT	**
E1BHN4	RING-type domain-containing protein	FLR	480.24	0.95	8.5	9.75	NT	*+
		FPH	450.22	0.94	8.56	6.74	NT	+*
		FRE	562.32	0.6	6	6	NT	**
		PHL	584.26	0.61	7.98	7.17	NT	+*
		PYR	496.24	0.73	9.14	9.18	NT	**
		RFG	434.26	0.96	6.25	9.75	NT	**
		YVF	434.23	0.71	11.32	5.52	NT	*+
F1MF78	Spectrin repeat containing nuclear envelope protein 2	LFH	418.24	0.85	8.39	6.74	NT	+*
		LHF	477.26	0.85	8.39	6.74	NT	**
		LLF	392.21	0.94	11.47	5.52	NT	*+
		LQF	488.29	0.81	7.63	5.52	NT	+*
		LRY	415.22	0.51	8.96	8.75	NT	**
		LSF	434.26	0.83	8.7	5.52	NT	**
		PFQ	445.23	0.9	7.77	5.96	NT	+*
		PLY	354.19	0.73	12.18	5.95	NT	**
		RFL	365.2	0.96	8.5	9.75	NT	**
		RLF	478.29	0.95	8.5	9.75	NT	**
		RLM	450.26	0.79	6.39	9.75	NT	**
		WEL	446.22	0.61	9.48	4	NT	**
		WKK	460.28	0.51	9.56	10	NT	**
		WLQ	501.3	0.82	8.6	5.52	NT	*+
		WRK	391.25	0.81	8.22	11	NT	**
		YWK	367.15	0.78	11.42	8.59	NT	**
F1MJJ0	Dynein axonemal heavy chain 9	FRF	359.16	1	8.96	9.75	NT	*+
		FRT	422.23	0.78	6.12	9.75	NT	+*
		HFA	373.18	0.71	6.51	6.74	NT	+*
		HGF	447.22	0.94	6	6.74	NT	**
		VHF	547.35	0.56	7.44	6.71	NT	**
		WHL	454.23	0.91	9.28	6.74	NT	+*
		WPH	438.2	0.95	9.47	6.74	NT	**
		WRP	457.24	0.98	9.53	9.75	NT	*+
		WSR	416.21	0.85	6.96	9.75	NT	*+
F1N0A6	Adhesion G protein-coupled receptor V1	WLW	496.23	0.99	12.83	5.52	NT	+*
		WPR	531.25	0.98	9.53	9.75	NT	**
P02662	Alpha-S1-casein	LFR	434.26	0.94	8.5	9.75	NT	+*
		LRF	468.25	0.95	8.5	9.75	NT	*+
		LRL	547.35	0.56	7.97	9.75	NT	**
		PLW	646.31	0.98	12.44	5.96	NT	*+
		RFF	488.23	0.99	8.96	9.75	NT	**
		RYL	351.18	0.56	8.96	8.75	NT	*+
		YLG	717.3	0.64	9.98	5.52	NT	+*
P02663	Alpha-S2-casein	NFL	528.27	0.89	8.04	5.52	NT	**
		NPW	560.28	0.95	9.2	5.52	NT	**
		YLY	457.22	0.54	12.42	5.52	NT	**
P02666	Beta-casein	AFL	550.22	0.93	9.83	5.57	NT	*+
		HLP	532.26	0.58	7.98	6.74	NT	+*
		HPF	365.21	0.95	8.56	6.74	NT	**
		KFQ	422.16	0.52	6.38	8.75	NT	**
		LLY	618.28	0.5	11.87	5.52	NT	**
		PPF	575.34	0.99	12.13	5.96	NT	**
		SWM	524.26	0.96	8.04	5.24	NT	**

"*" indicates that the peptide was detected in the sample, and "+" indicates that the peptide was not detected in the sample.

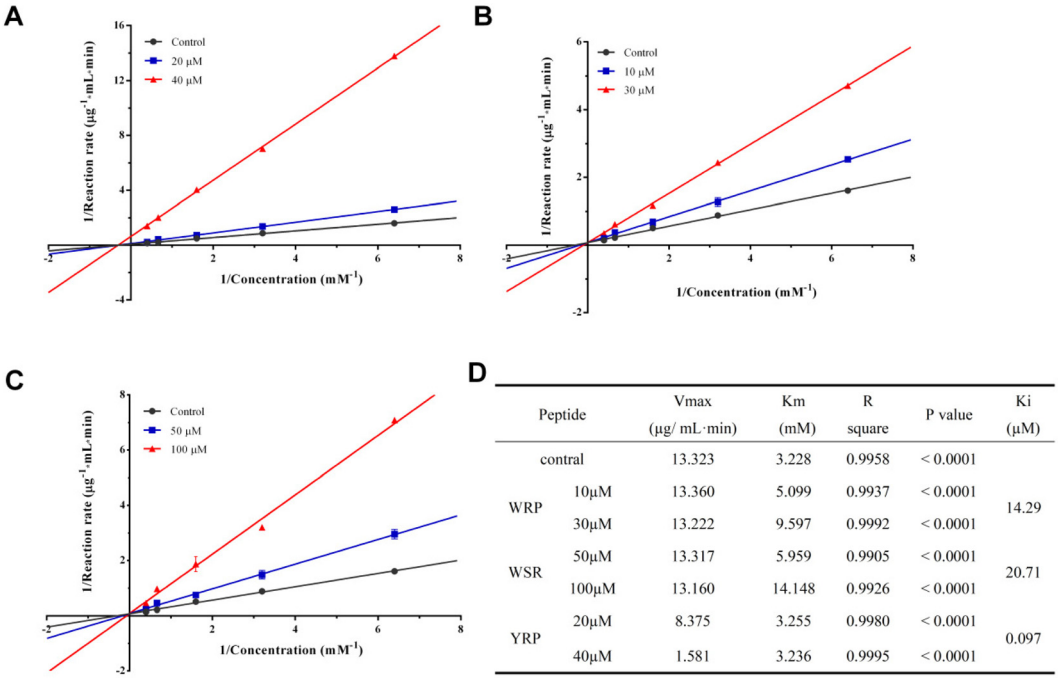

D

Peptide		Vmax (μg/ mL·min)	Km (mM)	R square	P value	Ki (μM)
contral		13.323	3.228	0.9958	< 0.0001	
WRP	10μM	13.360	5.099	0.9937	< 0.0001	14.29
	30μM	13.222	9.597	0.9992	< 0.0001	
WSR	50μM	13.317	5.959	0.9905	< 0.0001	20.71
	100μM	13.160	14.148	0.9926	< 0.0001	
YRP	20μM	8.375	3.255	0.9980	< 0.0001	0.097
	40μM	1.581	3.236	0.9995	< 0.0001	

Fig. 2 Lineweaver–Burk diagram of tripeptides obtained from FM and UHP-FM (A: YRP; B: WRP; C: WSR; D: kinetic parameters of ACE-catalyzed reactions at different concentrations of short peptides).

together to simulate physiological digestion. The changes in the biological activities of these peptides were then detected. After WSR was treated with pepsin, trypsin, and gastrointestinal protease (Fig. 3), its ACE inhibitory activity decreased significantly ($P > 0.05$). The original ACE inhibition rate of WRP was 98.50 ± 1.3% and did not change significantly after treatment with pepsin, trypsin, and gastrointestinal protease ($P < 0.05$) (ACE inhibition rates of 98.15 ± 0.65%, 97.75 ± 0.44%, and 98.34 ± 0.14%, respectively). The original ACE inhibitory rate of YRP was 98.18 ± 0.12%, and it decreased to 95.96 ± 0.09% and 97.39 ± 0.82% after treatment with pepsin and trypsin, respectively, showing no significant difference ($P < 0.05$). However, after treatment with gastrointestinal protease, the ACE inhibitory activity of YRP reduced significantly ($P > 0.05$), reaching 95.92 ± 0.84%. Peptides are absorbed through the small intestine and then enter the body's circulation, reaching various cells, tissues, and organs.[30] The systemic delivery of biologics *via* the gastrointestinal tract remains a substantial challenge.[31,32] Nevertheless, our findings show that the tripeptides WRP and YRP have good gastrointestinal stability. Hence, in order to achieve better peptide absorption and targeting, molecular modification or embedding approaches based on these sequences can be used. This could improve the stability and absorbability of biologics in the gastrointestinal tract.[30]

3.4 Probing binding sites using molecular docking

-CDOCKER_ENERGY and -CDOCKER_INTERNATION_ENERGY are indicators of the quality of molecular docking results. -CDOCKER_ENERGY is calculated based on the strain energy of the internal ligand. Meanwhile, -CDOCKER_NTERNATION_ENERGY is the energy of the receptor–ligand interaction, which represents the energy of the non-bond interaction that exists between the protein and ligand. High values of these two indicators suggest good ligand–receptor interaction (good binding between the protein and ligand). In this study, the position with the highest values for these two indicators was selected for further analysis as the optimal binding position. The docking results for the peptides and ACE are shown in Table 2.

ACE mainly consists of three active site pockets—S1′, S1, and S2. The S1′ pocket is considered the main pocket for the interaction between ACE and peptides and has only one amino acid residue, Glu162.[33] The S1 pocket consists of three amino acid residues (Glu384, Ala354, and Tyr523), whereas the S2 pocket contains five amino acid residues (His383, Gln281, Tyr520, Gln282, and Lys511). Glu411, His383, and His387 play an important role in the interaction at the inhibition site. In addition, Zn^{2+} is vital for the docking process.[34]

As shown in Fig. 4A, WRP forms a carbon–hydrogen bond with the ACE amino acid residue $His387_{2.97\ Å}$, and its bond angle is 92.78°. This region is one of the active sites of ACE. WRP and $Val518_{4.78\ Å}$ show alkyl hydrophobic interactions, whereas WRP shows electrostatic interactions with $Zn701_{2.22\ Å}$ and $ASP358_{5.40\ Å}$ and π–anion electrostatic interactions with $Glu403_{3.77\ Å}$. WRP exhibits van der Waals interactions with His383, Ala354, Ser355, Tyr523, Ala356, Trp357, Phe391, Tyr394, Arg402, Tyr360, Trp59, Lys118, Met223, Pro407, Gly404, Arg522, and Glu411.

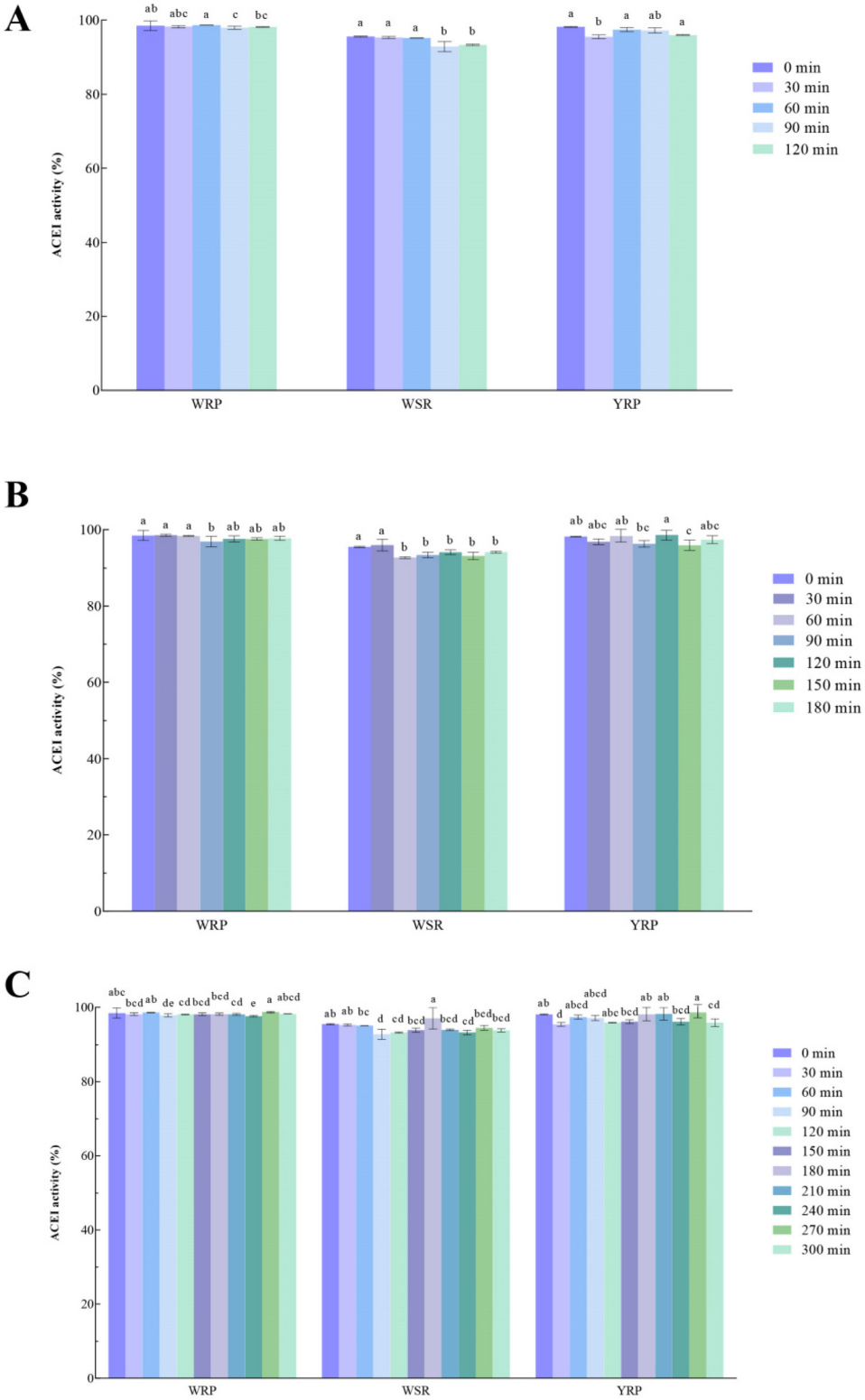

Fig. 3 Validation of gastrointestinal stability of fermented milk-derived ACE inhibitory peptides (A: pepsin digestion: B: trypsin digestion; C: gastrointestinal protease digestion).

As demonstrated in Fig. 4B, WSR and the amino acid residues Tyr $523_{2.43}$ Å and $Ala354_{2.43}$ Å of ACE form two conventional hydrogen bonds with different distances and bond angles of 130.695° and 130.949°, respectively. Both of them are located in the S1 pocket, and the force is thus strong. His387 is one of the active sites of ACE, and WSR forms a carbon–

Table 2 Results of flexible docking interactions between the tripeptides and ACE

	ChiRotor *E*-total (kcal mol^{-1})	ChiRotor *E*-elec (kcal mol^{-1})	ChiRotor *E*-vdw (kcal mol^{-1})	ChiFlex Energr (kcal mol^{-1})	CDOCKE_ENERGY (kcal mol^{-1})	CDOCKER_INTERATION_ENERGY (kcal mol^{-1})
WRP	−46.22	−8.19	−48.69	9.13	−73.7	−90.31
WSR	−45.44	−9.31	−48.03	−8.32	−80.97	−85.6
YRP	−41.48	−7.28	−46.95	9.13	−78.91	−93.67

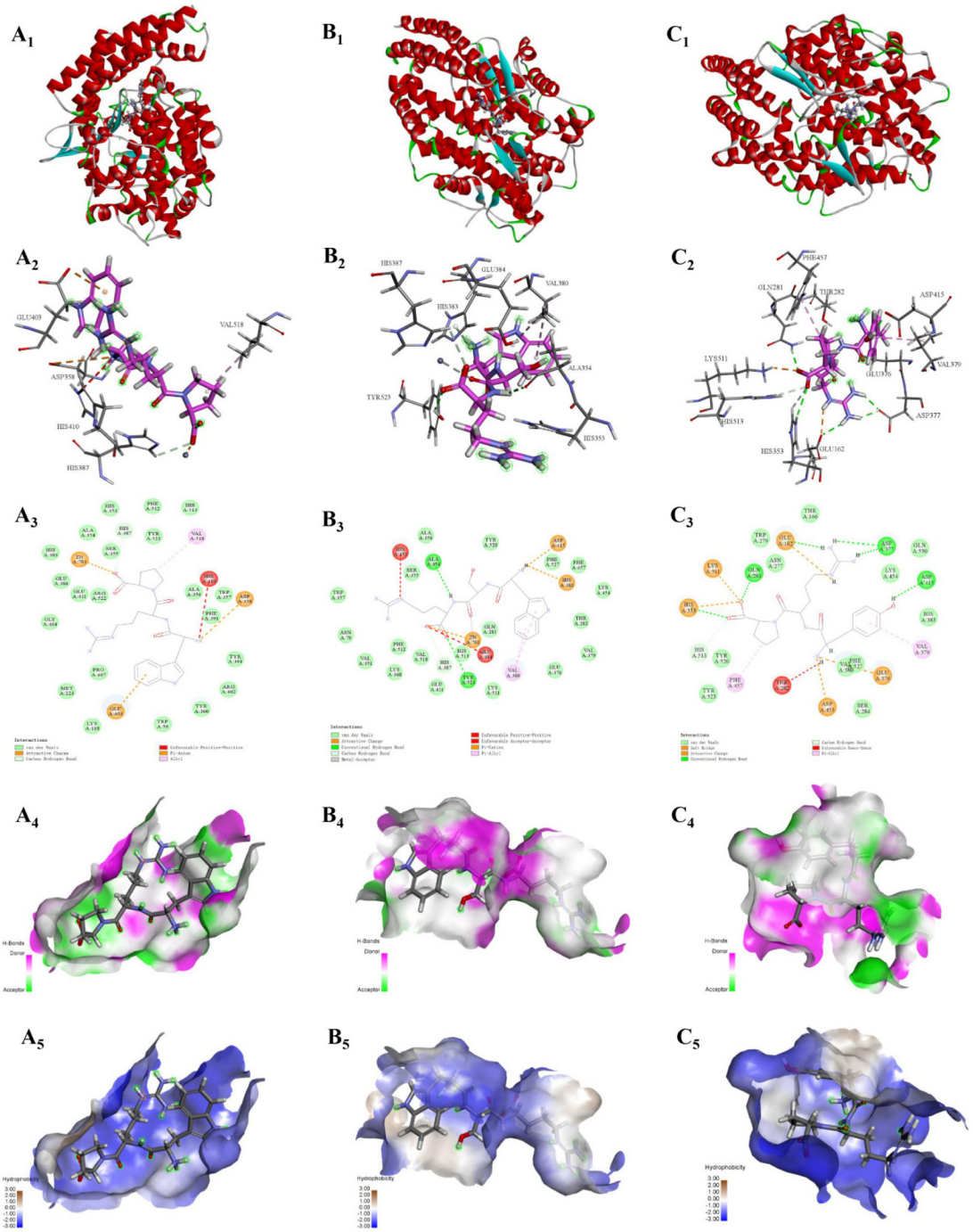

Fig. 4 Molecular docking models of YRP (A), WSR (B), and WRP (C) with angiotensin converting enzyme. (A_1, B_1, and C_1: 3D overall docking of tripeptides to the molecule ACE; A_2, B_2, and C_2: 3D diagram of local interaction between tripeptides and ACE amino acid residues; A_3, B_3, and C_3: 2D interaction diagram of tripeptides with the amino acid residues of ACE; A_4, B_4, and C_4: 3D H-bond interaction diagram of tripeptides with ACE amino acid residues; A_5, B_5, and C_5: 3D hydrophobic interaction diagram of tripeptides with ACE amino acid residues.)

hydrogen bond with $His387_{2.99\ Å}$ at a bond angle of 96.483°. WSR and $VAL380_{5.41/5.05\ Å}$ show π–alkyl hydrophobic interactions, and WSR reacts with $Zn701_{2.90\ Å}$ to form a metal receptor. WSR forms electrostatic interactions with $Zn701_{2.24\ Å}$ and $Asp415_{4.46\ Å}$, and WSR and $His383_{2.72\ Å}$ show π–cation electrostatic interactions. Moreover, WSR exhibits van der Waals interactions with Trp357, Ser355, Ala356, Tyr520, Phe527, Phe457, Lys454, Thr282, Val379, Glu376, Lys511, Gln281, His513, His387, Glu411, Val519, Phe512, Lys368, Val351, and Asn70.

Fig. 4C shows that YRP forms six conventional hydrogen bonds with the ACE amino acid residues $Gln281_{2.05\ Å}$, $His353_{2.75\ Å}$, $Asp415_{1.98\ Å}$, $Glu162_{2.25\ Å}$, and $Asp377_{2.05/2.10\ Å}$, with bond angles of 144.433°, 118.163°, 153.979°, 153.713°, 148.343°, and 146.219°, respectively. YRP forms three carbon–hydrogen bonds with $His353_{2.84\ Å}$, $His513_{2.70\ Å}$, and $Glu376_{3.04\ Å}$, at bond angles of 110.587°, 133.244° and 118.828°, respectively. YRP shows π–alkyl hydrophobic interactions with $Phe457_{4.63\ Å}$ and $Val379_{4.83\ Å}$ and forms a salt bridge with $Lys511_{2.41\ Å}$ and $Glu162_{2.59\ Å}$. YRP shows electrostatic interactions with $His353_{4.76\ Å}$, $Glu376_{4.19\ Å}$, and $Asp453_{3.18\ Å}$. YRP also interacts with Trp279, Thr166, Lys454, Glu530, His383, Val380, Phe527, Ser284, Tyr523, Tyr520, and Asn277 *via* van der Waals forces. YRP interacts with the Gln281, His353, His513, and Lys511 in the S2 pocket of ACE and forms a hydrogen bond and salt bridge with Glu162 in the S1′ pocket.

3.5 MD simulation

3.5.1 Probing binding sites. The trajectories of the ACE protein backbone converged at approximately 20 and 15 ns. The RMSD values for the three systems fluctuated between 0.10 and 0.22 nm (Fig. 5A). The trajectories of all three peptides converged at approximately 40 ns, and the RMSD values fluctuated between 0.05 and 0.1 nm for WRP, WSR, and YRP (Fig. 5B). These data suggested that all three tripeptides could

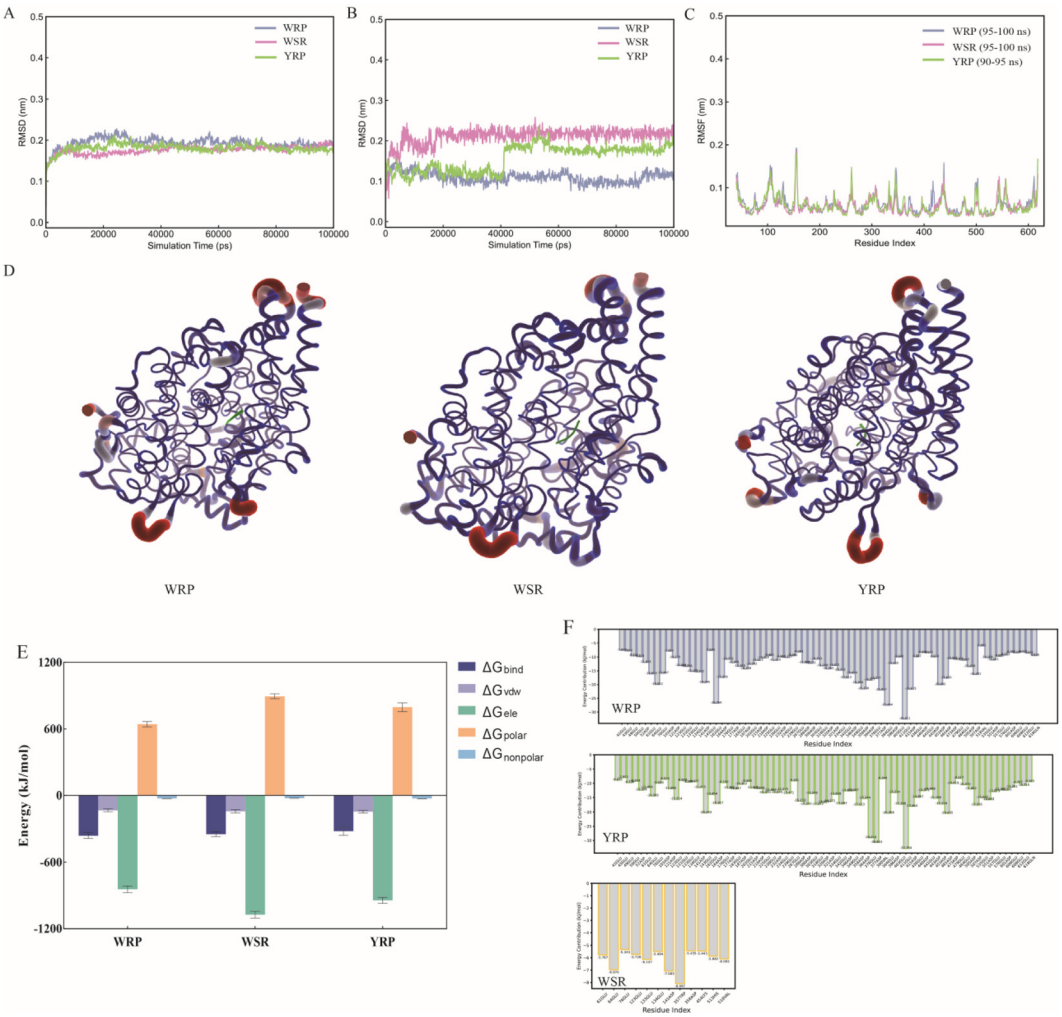

Fig. 5 RMSD, RMSF, β factor values, Binding free energy and hydrogen bond energy contribution obtained from the MD simulation of fermented milk-derived ACE inhibitory peptides (A: RMSD values of the three ACE-peptide systems; B: RMSD values of the three peptide systems; C: RMSF values of the three ACE-peptide systems; D: β-factor of the three ACE-peptide systems; E: binding free energy; F: hydrogen bond energy contribution).

stably bind to the active site. However, WSR and YRP exhibited especially large fluctuations. Meanwhile, ACE binding with WRP reached equilibrium faster than ACE binding with YRP or WSR, indicating that the interaction of ACE and WRP was more stable.[35]

RMSF plots indicated that all residues from the three ACE–peptide systems showed similar conformational fluctuations (Fig. 5C). Under the simulated conditions, the maximum RMSF value was also less than 0.5, indicating that ACE was relatively stable during complex formation.[36] During simulation, most fluctuations in the residues within the ACE ring were more flexible than those of the residues in the helical region. The representative stable structures at 100 ns (β-factor) indicated that the conformational fluctuations of the three systems were similar (Fig. 5D).

3.5.2 Binding mode of peptides. Free energy landscapes (FELs) were used to select the representative conformations of the three systems for binding mode analysis. The FELs were determined as a function of R_g (PC1) and RMSD (PC2), which revealed the local conformations with the lowest energy. As shown by the FELs in Fig. 6 (darker blue, lower energy), the reprehensive structures for the three systems were as follows: WRP (99.2 ns, Fig. 6A), YRP (94.0 ns, Fig. 6B), and WSR (91.6 ns, Fig. 6C). Binding mode analysis revealed that the three peptides exhibited stable bonds with ACE.

WRP formed five hydrogen bonds with $Leu139_{2.25}$ Å, $Glu143_{2.69}$ Å, $Glu411_{1.86/2.42}$ Å, and $Arg522_{1.73}$ Å; four hydrophobic interactions with $Leu81_{5.37}$ Å, $Leu140_{5.38}$ Å, $His410_{5.38}$ Å, and $Val518_{4.69}$ Å; and electrostatic interactions with $Glu143_{4.17}$ Å. The active site Glu411 had a stable effect. YRP formed six hydrogen bonds with $Gln281_{2.97}$ Å, $Glu384_{2.17/2.36/2.20}$ Å, $Lys511_{1.80}$ Å, and $His513_{2.51}$ Å; two hydrophobic interactions with $His353_{5.23}$ Å and $Val380_{4.98}$ Å; and electrostatic interactions with $Glu376_{4.47}$ Å. During simulation, YRP exerted relatively stable effects on Glu384 in the S1 pocket and Lys511, His513, His353, and Gln281 in the S2 pocket. WSR formed six hydrogen bonds with $Asn66_{1.81}$ Å, $Glu143_{2.09}$ Å, $His353_{1.93}$ Å, $His513_{1.92}$ Å, $Arg522_{2.83}$ Å, and $Tyr523_{2.32}$ Å and four hydrophobic interactions with $Trp357_{3.95/.36}$ Å, $His513_{4.56}$ Å, and $Val518_{4.94}$ Å. It showed an electrostatic charge interaction with $Glu143_{1.88}$ Å. During simulation, WSR exerted relatively stable effects on Tyr523 in the S1 pocket and His513 and His353 in the S2 pocket.

We studied the pattern of hydrogen bonds between the ACE protein and the three tripeptides. The number of hydrogen bonds formed between the three peptides and ACE was altered (Fig. 6D–F), and only the bonds that strictly met the hydrogen bond formation angle and distance criteria remained. The ACE–peptide systems formed after 40 ns were 4–11 for WRP hydrogen bonds, 7–15 for WSR hydrogen bonds, and 2–9 for YRP hydrogen bonds. These data indicated that the binding of the three peptides to the active sites of ACE was stable, and with WRP and WSR exhibiting the most stable binding.

3.5.3 Binding free energy calculation and decomposition. In this study, the binding free energies were effectively estimated using the MM-PBSA method. For each system, 51 snapshots were taken at intervals of 100 ps from the structural ensemble recorded in the MD trajectory during the last 5 ns. The ΔG_{bind} values are provided in Fig. 5E. The ΔG_{bind} values for WRP, WSR, and YRP were -360.7 ± 24.8 kJ mol^{-1}, $-346.3 \pm$

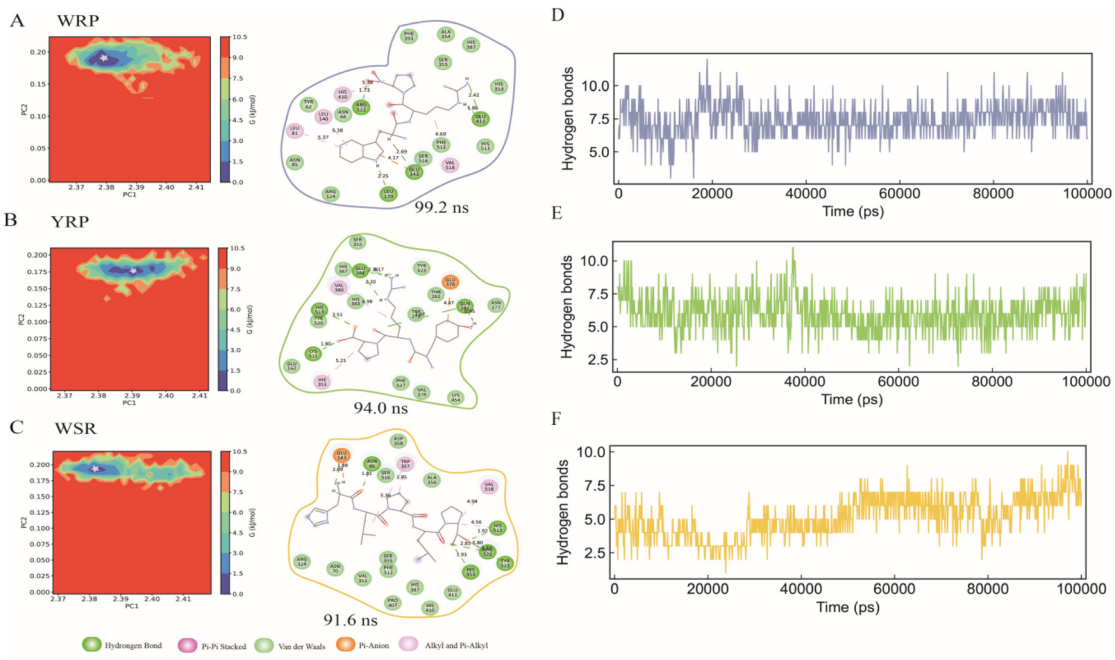

Fig. 6 Molecular dynamics of hydrogen bonds and the free-energy landscape of ACE inhibitory peptides derived from fermented milk. (A, B, and C: free-energy landscapes, docking results of tripeptides and ACE in molecular dynamics simulation; D, E, and F: hydrogen bonds in the molecular dynamics simulation of ACE inhibitory peptides from fermented milk.)

22.3 kJ mol^{-1}, and −320.0 ± 38.8 kJ mol^{-1}, respectively. WRP exhibited stronger interactions with ACE than WSR and YRP. ΔG_{bind} consists of ΔG_{vdw}, ΔG_{ele}, ΔG_{pol}, and ΔG_{nonpol}, among which ΔG_{vdw}, ΔG_{ele}, and ΔG_{nonpol}—but not ΔG_{pol}—were favorable to inhibitor binding.[37]

The contribution of different residues to ΔG_{bind} in the three systems was investigated *via* energy decomposition analysis. A residue was considered important for ligand binding if its interaction energy with the residue was <−1 kcal mol^{-1}. To identify the most important residues contributing to ΔG_{bind}, the energy threshold was set to −5 kcal mol^{-1}. In total, 71, 71, and 12 residues were found to be important for WRP, YRP, and WSR, respectively (Fig. 5F). Clearly, WRP, WSR, and YRP displayed stable interactions with the residues in the active site of the ACE protein. The free energy binding (ΔG) value of Captopril to ACE at 310 K calculated based on MM-PBSA was −14.89 kcal mol^{-1}.[38] Captopril was a small compound containing sulfhydryl group, and it was found that captopril forms hydrogen bond with amino acid Gln 281 His 353 Glu 384 His 513 Tyr 520 Lys 511, the active site of ACE.[39,40] The comparison shows that the results of molecular docking and molecular dynamics simulations of WRP, WSR and YRP were good, which can be further verified.

4. Conclusion

Peptides in milk fermented by *Lactobacillus delbrueckii* QS306 before and after ultra-high pressure treatment were identified in this study using proteomics. Among 566 short peptides, 170 new tripeptides were discovered. Of these, 75 tripeptides with potential ACE inhibitory activity were screened based on activity score prediction and hydrophobicity calculations, and 16 tripeptides with good stability were identified based on PeptideCutter analysis. WRP, WSR, and YRP exhibited the best inhibitory activities. WRP and WSR appeared to be competitive inhibitors, while YRP was non-competitive. Gastrointestinal simulation revealed that WRP and YRP have better gastrointestinal stability. The results of molecular docking showed that the distance between WRP and zinc ions was larger than that of YRP and zinc ions. The hydrophobicity of WRP was greater than that of YRP and WSR, and the sequence of WRP was similar to that of YRP. The amino acid side chain of WRP had a cyclic structure (tryptophan, phenylalanine, and proline), increasing the ACE inhibitory activity of the peptide. The values of RMSD, ΔG_{bind}, ΔG_{pol}, and RSMF obtained from the molecular dynamics simulation indicated that the combination of WRP and ACE was stable. Therefore, the antihypertensive mechanism of WRP should be studied in rat models of essential hypertension.

Author contributions

Nan Wu: conceptualization, data curation, formal analysis, methodology, project administration, resources, writing – original draft. Puyu Li: formal analysis, methodology, writing – original draft. Wuhanqimuge: conceptualization, data curation, resources, project administration. Quan Shuang: conceptualization, resources, project administration.

Conflicts of interest

The authors declare that they have no known competing financial interests or personal relationships that could appear to influence the work reported in this paper.

Acknowledgements

This work was supported by the Inner Mongolia Natural Science Foundation (grant no. 2021MS03059), Inner Mongolia Chinese and Mongolian Medicine Young and Middle Aged Leader Project (NEI WEI ZHONG (MENG) CHUAN CHENG ZI (2022) NO. 108), Inner Mongolia Young and Middle-aged Leading Talents Project (NEI WEI ZHONG (MENG) CHUAN CHENG ZI (2022) 88) and National Natural Science Foundation of China-Young Foundation (grant no. 82204377). We thank Shanghai Bioprofile Technology Company Ltd for peptide sequence analysis using UPLC-Q-exactive-HF-X-MS/MS.

References

1 I.-M. Chung, J.-K. Kim, I. Park, J.-Y. Oh and S.-H. Kim, Effects of milk type, production month, and brand on fatty acid composition: A case study in Korea, *Food Chem.*, 2016, **196**, 138–147.
2 J. Tuomilehto, J. Lindström, J. Hyyrynen, R. Korpela, M. L. Karhunen, L. Mikkola, T. Jauhiainen, L. Seppo and A. Nissinen, Effect of ingesting sour milk fermented using Lactobacillus helveticus bacteria producing tripeptides on blood pressure in subjects with mild hypertension, *J. Hum. Hypertens.*, 2004, **18**, 795–802.
3 F. Wang, Y. Zhang, T. Yu, J. He, J. Cui, J. Wang, X. Cheng and J. Fan, Oat globulin peptides regulate antidiabetic drug targets and glucose transporters in Caco-2 cells, *J. Funct. Foods*, 2018, **42**, 12–20.
4 M. L. Timón, A. I. Andrés, J. Otte and M. J. Petrón, Antioxidant peptides (<3 kDa) identified on hard cow milk cheese with rennet from different origin, *Food Res. Int.*, 2019, **120**, 643–649.
5 M. Mushtaq, A. Gani and F. A. Masoodi, Himalayan cheese (Kalari/Kradi) fermented with different probiotic strains: In vitro investigation of nutraceutical properties, *LWT–Food Sci. Technol.*, 2019, **104**, 53–60.
6 C. Adams, F. Sawh, J. M. Green-Johnson, H. Jones Taggart and J. L. Strap, Characterization of casein-derived peptide bioactivity: Differential effects on angiotensin-converting enzyme inhibition and cytokine and nitric oxide production, *J. Dairy Sci.*, 2020, **103**, 5805–5815.

7 M. Ezzati, A. D. Lopez, A. Rodgers, S. Vander Hoorn and C. J. Murray, Selected major risk factors and global and regional burden of disease, *Lancet*, 2002, **360**, 1347–1360.
8 D. T. Ko, P. R. Hebert, C. S. Coffey, J. P. Curtis, J. M. Foody, A. Sedrakyan and H. M. Krumholz, Adverse effects of beta-blocker therapy for patients with heart failure: a quantitative overview of randomized trials, *Arch. Intern. Med.*, 2004, **164**, 1389–1394.
9 N. J. Brown and D. E. Vaughan, Angiotensin-converting enzyme inhibitors, *Circulation*, 1998, **97**, 1411–1420.
10 S. H. Ferreira, D. C. Bartelt and L. J. Greene, Isolation of bradykinin-potentiating peptides from Bothrops jararaca venom, *Biochemistry*, 1970, **9**, 2583–2593.
11 D. Pan, Y. Luo and M. Tanokura, Antihypertensive peptides from skimmed milk hydrolysate digested by cell-free extract of *Lactobacillus helveticus*, JCM1004, *Food Chem.*, 2005, **91**, 123–129.
12 F. Giacometti Cavalheiro, D. Parra Baptista, B. Domingues Galli, F. Negrão, M. Nogueira Eberlin and M. Lúcia Gigante, High protein yogurt with addition of Lactobacillus helveticus: Peptide profile and angiotensin-converting enzyme ACE-inhibitory activity, *Food Chem.*, 2020, **333**, 127482.
13 B. Singh, R. Chand and R. Singh, Angiotensin-1 converting enzyme (ACE) inhibitory activity of peptides isolated from bovine milk fermented with Lactobacillus helveticus NCDC-288, *Milchwissenschaft*, 2011, **66**, 429–432.
14 D. Solanki, A. Sakure, S. Prakash and S. Hati, Characterization of Angiotensin I-Converting Enzyme (ACE) inhibitory peptides produced in fermented camel milk (Indian breed) by Lactobacillus acidophilus NCDC-15, *J. Food Sci. Technol.*, 2022, **59**, 3567–3577.
15 G. Shu, X. Shi, H. Chen, Z. Ji and J. Meng, Optimization of Nutrient Composition for Producing ACE Inhibitory Peptides from Goat Milk Fermented by Lactobacillus bulgaricus LB6, *Probiotics Antimicrob. Proteins*, 2019, **11**, 723–729.
16 J. Sebastián-Nicolás, E. Lopez, J. Ramirez, A. Cruz, G. Rodríguez-Serrano, J. Añorve Morga, J. Jaimez, A. Castañeda, E. Pérez-Escalante, A. Ayala-Niño and L. González-olivares, Milk Fermentation by Lacticaseibacillus rhamnosus GG and Streptococcus thermophilus SY-102: Proteolytic Profile and ACE-Inhibitory Activity, *Fermentation*, 2021, **7**, 215.
17 P. Mudgil, C.-Y. Gan, M. Affan Baig, M. Hamdi, K. Mohteshamuddin, J. E. Aguilar-Toalá, A. M. Vidal-Limon, A. M. Liceaga and S. Maqsood, In-depth peptidomic profile and molecular simulation studies on ACE-inhibitory peptides derived from probiotic fermented milk of different farm animals, *Food Res. Int.*, 2023, **168**, 112706.
18 M. Tu, S. Cheng, W. Lu and M. Du, Advancement and prospects of bioinformatics analysis for studying bioactive peptides from food-derived protein: Sequence, structure, and functions, *TrAC, Trends Anal. Chem.*, 2018, **105**, 7–17.
19 J. Caballero, Considerations for Docking of Selective Angiotensin-Converting Enzyme Inhibitors, *Molecules*, 2020, **25**(2), 295.
20 N. Wu, Y. Zhao, Y. Wang and Q. Shuang, Effects of ultra-high pressure treatment on angiotensin-converting enzyme (ACE) inhibitory activity, antioxidant activity, and physicochemical properties of milk fermented with Lactobacillus delbrueckii QS306, *J. Dairy Sci.*, 2022, **105**, 1837–1847.
21 J. Cox, N. Neuhauser, A. Michalski, R. A. Scheltema, J. V. Olsen and M. Mann, Andromeda: a peptide search engine integrated into the MaxQuant environment, *J. Proteome Res.*, 2011, **10**, 1794–1805.
22 N. Wu, F. Zhang and Q. Shuang, Peptidomic analysis of the angiotensin-converting-enzyme inhibitory peptides in milk fermented with Lactobacillus delbrueckii QS306 after ultra-high pressure treatment, *Food Res. Int.*, 2023, **164**, 112406.
23 M.-L. Sun, Q. Zhang, Q. Ma, Y.-H. Fu, W.-G. Jin and B.-W. Zhu, Affinity purification of angiotensin-converting enzyme inhibitory peptides from Volutharpa ampullacea perryi protein hydrolysate using Zn-SBA-15 immobilized ACE, *Eur. Food Res. Technol.*, 2018, **244**, 457–468.
24 C.-Z. Zhu, W.-G. Zhang, Z.-L. Kang, G.-H. Zhou and X.-L. Xu, Stability of an antioxidant peptide extracted from Jinhua ham, *Meat Sci.*, 2014, **96**, 783–789.
25 J. E. Garbarino and I. R. Gibbons, Expression and genomic analysis of midasin, a novel and highly conserved AAA protein distantly related to dynein, *BMC Genomics*, 2002, **3**, 18.
26 K. E. Bernstein, X. Z. Shen, R. A. Gonzalez-Villalobos, S. Billet, D. Okwan-Duodu, F. S. Ong and S. Fuchs, Different in vivo functions of the two catalytic domains of angiotensin-converting enzyme (ACE), *Curr. Opin. Pharmacol.*, 2011, **11**, 105–111.
27 S. M. Auwal, N. Zarei Abidin, M. Zarei, C. P. Tan and N. Saari, Identification, structure-activity relationship and in silico molecular docking analyses of five novel angiotensin I-converting enzyme (ACE)-inhibitory peptides from stone fish (Actinopyga lecanora) hydrolysates, *PLoS One*, 2019, **14**(5), e0197644.
28 J.-Y. Ko, N. Kang, J.-H. Lee, J.-S. Kim, W.-S. Kim, S.-J. Park, Y.-T. Kim and Y.-J. Jeon, Angiotensin I-converting enzyme inhibitory peptides from an enzymatic hydrolysate of flounder fish (Paralichthys olivaceus) muscle as a potent anti-hypertensive agent, *Process Biochem.*, 2016, **51**, 535–541.
29 M. Guo, X. Chen, Y. Wu, L. Zhang, W. Huang, Y. Yuan, M. Fang, J. Xie and D. Wei, Angiotensin I-converting enzyme inhibitory peptides from Sipuncula (Phascolosoma esculenta): Purification, identification, molecular docking and antihypertensive effects on spontaneously hypertensive rats, *Process Biochem.*, 2017, **63**, 84–95.
30 W. Shen and T. Matsui, Intestinal absorption of small peptides: a review, *Int. J. Food Sci. Technol.*, 2019, **54**, 1942–1948.
31 D. J. Brayden, T. A. Hill, D. P. Fairlie, S. Maher and R. J. Mrsny, Systemic delivery of peptides by the oral route: Formulation and medicinal chemistry approaches, *Adv. Drug Delivery Rev.*, 2020, **157**, 2–36.
32 M. Durán-Lobato, Z. Niu and M. J. Alonso, Oral Delivery of Biologics for Precision Medicine, *Adv. Mater.*, 2020, **32**, e1901935.

33 Y. Y. Ngoh and C. Y. Gan, Identification of Pinto bean peptides with inhibitory effects on α-amylase and angiotensin converting enzyme (ACE) activities using an integrated bioinformatics-assisted approach, *Food Chem.*, 2018, **267**, 124–131.
34 X. Wang, S. Wu, D. Xu, D. Xie and H. Guo, Inhibitor and substrate binding by angiotensin-converting enzyme: quantum mechanical/molecular mechanical molecular dynamics studies, *J. Chem. Inf. Model.*, 2011, **51**, 1074–1082.
35 W. Yan, G. Lin, R. Zhang, Z. Liang, L. Wu and W. Wu, Studies on molecular mechanism between ACE and inhibitory peptides in different bioactivities by 3D-QSAR and MD simulations, *J. Mol. Liq.*, 2020, **304**, 112702.
36 X. Feng, D. Liao, L. Sun, S. Feng, S. Wu, P. Lan, Z. Wang and X. Lan, Exploration of interaction between angiotensin I-converting enzyme (ACE) and the inhibitory peptide from Wakame (Undaria pinnatifida), *Int. J. Biol. Macromol.*, 2022, **204**, 193–203.
37 H. Zhang, Q.-Q. Luo, M.-L. Hu, N. Wang, H.-Z. Qi, H.-R. Zhang and L. Ding, Discovery of potent microtubule-destabilizing agents targeting for colchicine site by virtual screening, biological evaluation, and molecular dynamics simulation, *Eur. J. Pharm. Sci.*, 2023, **180**, 106340.
38 M. A. Triputra and A. Yanuar, Analysis of Compounds Isolated from Gnetum gnemon L. Seeds as Potential ACE Inhibitors through Molecular Docking and Molecular Dynamics Simulations, *J. Young Pharm.*, 2018, **10**(2s), S32–S39.
39 M. Memarpoor-Yazdi, H. Zare-Zardini, N. Mogharrab and L. Navapour, Purification, Characterization and Mechanistic Evaluation of Angiotensin Converting Enzyme Inhibitory Peptides Derived from Zizyphus Jujuba Fruit, *Sci. Rep.*, 2020, **10**, 3976.
40 A. Limanto, E. E. F. Husain and A. M. Dewajanti, In-silico study of the Effectiveness of Allium sativum L. extract as an Angiotensin-Converting Enzyme (ACE) Inhibitor in Hypertension, *Maj. Kedokt. Bandung*, 2023, **55**(3), 161–170.